

Nonlinear Interaction of Waves in Rotating Spherical Layers

D Zhilenko¹, O Krivonosova¹ and M Gritsevich^{2,3,4}

¹ Moscow State University, GSP-1, Leninskie Gory, 119991, Moscow, Russia

² Department of Physics, University of Helsinki, Gustaf H  llstr  min katu 2a, FI-00014 Helsinki, Finland

³ Dorodnicyn Computing Center, RAS, Vavilova str. 40, 119333, Moscow, Russia

⁴ Institute of Physics and Technology, Ural Federal University, Mira str. 19, 620002, Ekaterinburg, Russia

E-mail: olga@imec.msu.ru

Abstract. Flows of a viscous incompressible fluid in a spherical layer that are due to rotational oscillations of its inner boundary at two frequencies with respect to the state of rest are numerically studied. It is found that an increase in the amplitude of oscillations of the boundary at the higher frequency can result in a significant enhancement of the low-frequency mode in a flow near the outer boundary. The direction of propagation of the low-frequency wave changes from radial to meridional, whereas the high-frequency wave propagates in the radial direction in a limited inner region of the spherical layer. The role of the meridional circulation in the energy exchange between spaced waves is demonstrated.

1. Introduction

Most of the flows in astrophysical objects (stars, planets, and atmospheres) are characterized by the spherical geometry and rotation. These factors can be taken into account in a model spherical Couette flow. Rotation is often nonuniform. The nonuniformity of rotation of the Sun and planets of the solar system is well studied (some data are presented, e.g., in [1]). In the first approximation, the nonuniformity of rotation can be represented as its periodic modulation. The periodic (single-frequency) modulation of the rotation velocity of one of the spherical boundaries in the case of their quite fast unidirectional rotation can result in the formation of inertial waves in a flow between these boundaries [2]. In the case of the absence of average rotation and small amplitudes, the rotational oscillations of the inner sphere at a single frequency produce damping spherical waves [3]. However, the time dependence of the rotation velocity of natural objects can be more complex. In particular, data on the length of days on the Earth [4] indicate a cyclic process in which at least two frequencies or two characteristic time scales can be identified. This fact stimulates our interest in the two-frequency modulation of the rotation velocity. It is known that the interaction between two waves can enhance one of them [5]. Here we study the process of interaction between two waves, which is not masked by other phenomena. The possibility of the generalization of obtained results is discussed in Section 4.

2. Numerical methods and field of study

An isothermal flow of a viscous incompressible fluid is described by the Navier–Stokes and continuity equations:



Content from this work may be used under the terms of the [Creative Commons Attribution 3.0 licence](https://creativecommons.org/licenses/by/3.0/). Any further distribution of this work must maintain attribution to the author(s) and the title of the work, journal citation and DOI.

$$\frac{\partial U}{\partial t} = U \times \text{rot}U - \text{grad}\left(\frac{p}{\rho} + \frac{U^2}{2}\right) - \nu \text{rotrot}U, \text{div}U = 0,$$

where U , p , ν , and ρ are the velocity, pressure, viscosity, and density of the fluid, respectively. These equations were numerically solved in a spherical coordinate system where the impermeability and no-slip conditions for the azimuthal u_ϕ , radial u_r , and polar u_θ components of the velocity have the form $u_\phi(r = r_{1,2}) = \Omega_{1,2}(t)r_{1,2}\sin\theta$, $u_r(r = r_{1,2}) = 0$, $u_\theta(r = r_{1,2}) = 0$, where subscripts 1 and 2 correspond to the inner and outer spheres, respectively. We used an algorithm of numerical solution [6] based on a conservative finite difference scheme of the discretization of the Navier – Stokes equations in space and a third-order semi-implicit Runge–Kutta scheme for integration in time. The applicability of axisymmetric approximation was confirmed by three-dimensional calculations. Discretization in space was performed on grids uniform in r and θ with the total number of nodes 4.8×10^4 . The sensitivity of the results to the parameters of a grid was analyzed, e.g., in [7]. Agreement between experimental results and calculations was achieved with stationary [8] and periodic [9] boundary conditions.

In this work, the structure of a flow formed under the action of oscillations of the inner boundary of the layer is also analyzed by plotting wave surfaces or equal-phase surfaces. To calculate the phase of a flow at each point of the layer as a function of time, we used an approach well known in radio physics [10]. In this approach, the real time series $x(t)$ is considered as a projection of the complex vector $Z(t)$ on the abscissa axis $x(t) = B(t)\cos\Phi(t)$, where $B(t)$ and $\Phi(t)$ are the amplitude and phase of the initial signal $x(t)$. One of the methods for determining the vector $Z(t)$ is as follows: $Z(t) = x(t) + i\dot{y}(t)$, $y(t) = H[x(t)] = \int_{-\infty}^{\infty} H(t-\tau)x(\tau)d\tau$, and $H(t) = (\pi t)^{-1}$ is the Hilbert transform; in this case

$B(t) = (x^2(t) + y^2(t))^{1/2}$, $\Phi(t) = \arctg(y(t)/x(t))$. When $x(t) = C \sin \omega t$ $B(t) = C$ and $\Phi(t) = \omega t$. Such an approach allows calculating the amplitude and phase of an arbitrary real signal, including a two-frequency signal, as functions of time. In this work, such a method was used to calculate the phase of the azimuthal component u_ϕ of the velocity at each point of the layer $\Psi(t, r, \theta)$ and phase of rotation of the oscillating sphere $\Psi_s(t)$. It was shown in [3] that the described method for analyzing the structure of the flow makes it possible to adequately reproduce inertial waves previously obtained in experiments and numerical calculations.

It was also demonstrated in [3] that harmonic oscillations of the inner sphere with small amplitudes generate radially damping spherical waves (figure 1a). The distance between phase jumps along radii coincides with half of the wavelength λ , which is calculated as the wavelength $\lambda = 2\pi\delta = 2\pi(\nu/\pi f)^{1/2}$ in the Stokes problem on a flow generated by harmonic oscillations of an infinite plate at the frequency f [11], δ is the thickness of the dynamic boundary layer. When the amplitude of oscillations of the sphere increases, the flow becomes complicated (figure 1b), and wave surfaces ending at the outer boundary appear, as well as nodes at which the azimuthal component of the flow is always zero.

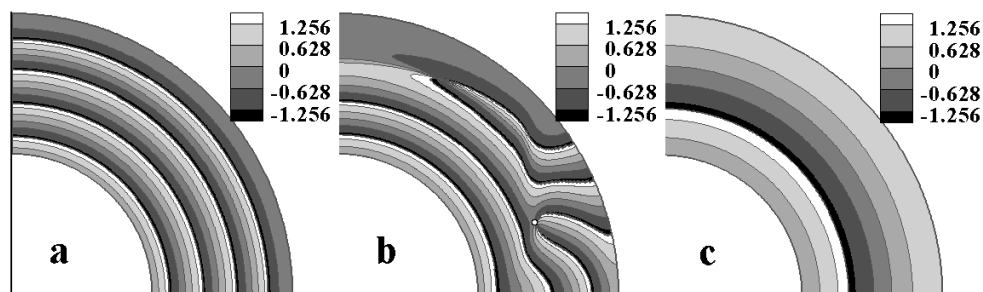


Figure 1. Wave surfaces (a) - $A=1s^{-1}$, $f=0.5s^{-1}$, (b) - $A=5s^{-1}$, $f=0.5s^{-1}$, (c) - $A=0.2s^{-1}$, $f=0.07s^{-1}$.

The rotational velocity of the inner sphere $\Omega(t)$ (the subscript 1 is omitted because $\Omega_2(t) = 0$ in this work) varies according to the law $\Omega(t) = A_1\sin(2\pi f_1 t) + A_2\sin(2\pi f_2 t)$, where the subscripts 1 and 2 refer

to the high- and low-frequency modes such that $f_2 < f_1$ and $A_2 < A_1$: $f_1 = 0.5 \text{ s}^{-1}$, $A_1 = 1$ and 5 s^{-1} and $f_2 = 0.07 \text{ s}^{-1}$, $A_2 = 0.2 \text{ s}^{-1}$. Calculations were performed with the dimensional parameters $r_1 = 0.075 \text{ m}$, $r_2 = 0.15 \text{ m}$ ($\sigma = (r_2 - r_1) / r_1 = 1$) and $\nu = 5 \times 10^{-5} \text{ m}^2 \text{ s}^{-1}$. At these parameters, the flow is unsteady and axisymmetric and there are no other frequencies except for the frequencies f_1 and f_2 in the azimuthal velocity spectrum.

3. Results

At first we consider the structure of the flow at small-amplitude oscillations of the inner boundary. Amplitudes are considered as small when spherical waves propagating in the radial direction appear (figure 1a,c, figure 2a). While $\Omega(t) = A \sin(2\pi f t)$, the phase shift $\psi_0(r, \theta) = \Psi(t, r, \theta) - \Psi_s(t)$ at the point with the coordinates (r, θ) with respect to the phase of oscillations of the boundary ($\Psi_s(t) = 2\pi f t$) is independent of the time [3]. Figure 2a shows the wave surfaces $\Psi(t_3, r, \theta)$ at a certain time instant t_3 (shown in figure 3c) at two-frequency small-amplitude oscillations. These surfaces are also attributed to a spherical wave, but the spherical layer in this case can be divided into three sublayers: a sublayer adjacent to the inner sphere where $\Psi(t_3, r, \theta) > 41$, a sublayer adjacent to the outer sphere where $\Psi(t_3, r, \theta) < 9.5$, and a narrow transient layer (shown in figure 2a in white) with a large phase gradient $9.5 < \Psi(t_3, r, \theta) < 41$, which increases in time (figure 2c shows the dependence of the phase of oscillations on the radius in the equatorial plane for three time instants, where the transient layer is shown in gray). The effective frequency \tilde{f} introduced as $2\pi\tilde{f}(t_2 - t_1) = \Psi(t_2, r, \theta) - \Psi(t_1, r, \theta)$ is $\tilde{f} \cong f_1$ in the inner sublayer, $\tilde{f} \cong f_2$ in the outer sublayer, and $f_2 < \tilde{f} < f_1$ in the transient sublayer. Figures 3a–c show the time dependence of the dimensionless azimuthal component of the velocity $u_\phi / |u_{\phi \max}|$, phase $\Psi(t, r, \theta)$ and its linear approximation at three points lying in each sublayer. It is seen that the rate of phase increase, i.e., the effective frequency \tilde{f} , varies depending on the character of variation of u_ϕ . The closer the time dependence of the velocity to harmonic oscillations, the closer the dependence $\Psi(t, r, \theta)$ to a linear time function and the closer the frequency \tilde{f} to the frequency of harmonic oscillations.

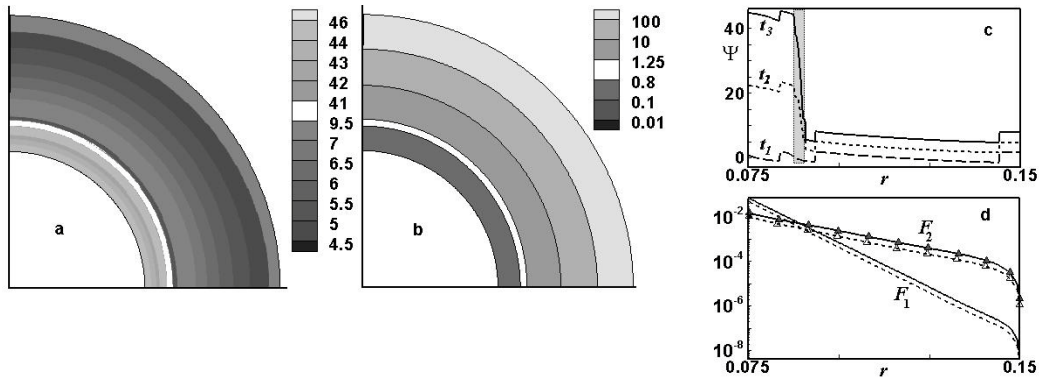


Figure 2. Two-frequency oscillations: $f_1 = 0.5 \text{ s}^{-1}$, $A_1 = 1 \text{ s}^{-1}$ and $f_2 = 0.07 \text{ s}^{-1}$, $A_2 = 0.2 \text{ s}^{-1}$. (a) - $\Psi(t_3, r, \theta)$, (b) - F_2 / F_1 , (c) - $\Psi(t, r, \theta = \pi/2)$, (d) - $F_1(r)$ and $F_2(r)$ at $\theta = \pi/2$ - solid lines and $\theta = \pi/4$ - dashed lines.

The ratio of the amplitudes F_2 and F_1 of the low- and high-frequency oscillation modes, respectively, at each point of the layer calculated using the Fourier transform in the transient region is in the interval $0.8 < F_2 / F_1 < 1.25$ (Figure 2b). Figure 2d shows the dependence of the amplitudes F_1 and F_2 on the radius at two values of the meridional angle: at the equator and at an angle of 45° to the rotation axis. The amplitudes F_1 and F_2 decrease exponentially as $\exp(-kr)$ in most of the thickness of the layer and the damping ratio k is independent of the meridional angle. The damping ratio k increases with the frequency ($k_1 = 184.5 \text{ m}^{-1}$, $k_2 = 75.24 \text{ m}^{-1}$); i.e., the high-frequency mode damps more

rapidly. As a result, a larger contribution to the flow near the inner sphere comes from the high-frequency mode, but it damps more rapidly, whereas the low-frequency mode makes a larger contribution to the flow behind the transient layer, where the amplitudes of the modes become closer to each other. The ratios of the amplitudes and the dependences of the amplitudes on the radius (see Figure 2b, d) coincide for the considered two-frequency oscillations and for two harmonic oscillations of the inner sphere (see Figure 1a, c); i.e., the modes of two-frequency small-amplitude oscillations do not interact with each other.

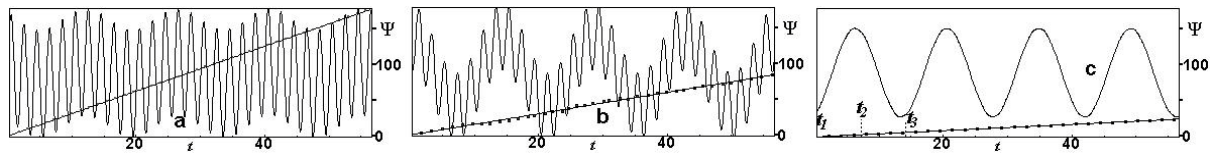


Figure 3. $u_\varphi/u_{\varphi \max}$ (sinusoids), Ψ (squares) and its linear approximations (straight lines) (a) - in the inner $r = 0.0752\text{m}$, (b) - in the transient $r = 0.09\text{m}$, and (c) - in the outer $r = 0.132\text{m}$ sublayers.

We now consider how the structure of the flow changes when the amplitude of only the high-frequency mode increases $A_1 = 5\text{s}^{-1}$ (figure 4). The spherical layer can also be divided into three regions (figure 4a). The first region is adjacent to the inner sphere, but its boundary has now a convexity near the equatorial plane. In this region, oscillations in time occur at \tilde{f} close to f_1 . The region adjacent to the outer sphere is characterized not only by oscillations at $\tilde{f} \equiv f_2$ but also by a change in the direction of propagation of waves from the radial direction to the meridional direction. Wave surfaces in this region are almost perpendicular to the outer sphere. Figure 4b shows zero u_φ contours at time instants, corresponding to maximal deviation of oscillating sphere. It is seen that these contours in the inner region are close to circles, whereas contours in the outer region are arranged in the radial direction. The comparison of images in Figure 4a, b indicates that the form of wave structures completely corresponds to the velocity field. The third transient region where $f_2 < \tilde{f} < f_1$ is between the inner and outer regions (white colour in figure 4a).

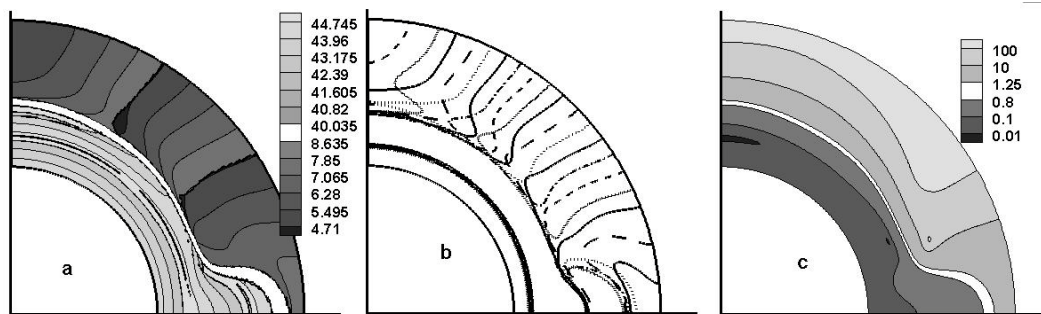


Figure 4. Two-frequency oscillations: $f_1 = 0.5\text{s}^{-1}$, $A_1 = 5\text{s}^{-1}$, $f_2 = 0.07\text{s}^{-1}$, $A_2 = 0.2\text{s}^{-1}$. (a) - $\Psi(t, r, \theta)$, (b) - contours $u_\varphi = 0$, (c) - F_2/F_1 .

The amplitudes F_1 and F_2 of the high- and low-frequency modes calculated using the Fourier transform in the transient region are close to each other (figure 4c). The dependences of the amplitudes on the radius in this case are shown in figure 5a. Figure 5b shows the amplitudes F_1 and F_2 calculated for harmonic oscillations of the sphere with the parameters of the high-frequency mode ($A_1 = 5\text{s}^{-1}$, $f_1 = 0.5\text{s}^{-1}$) and low-frequency mode ($A_1 = 0.02\text{s}^{-1}$, $f_1 = 0.07\text{s}^{-1}$). At $A_1 = 5\text{s}^{-1}$, high-frequency oscillations cannot be treated as small-amplitude and the structure of wave surfaces changes (cf. figure 1a, b).

The damping ratio determined from the dependence $F_1(r)$ (figure 5b) depends on the meridional angle. In the equatorial plane, $k_1(\pi/2) = 63.6\text{m}^{-1}$ is almost one third of the value $k_1 = 184.5\text{m}^{-1}$ at small-amplitude oscillations (figure 2d), whereas the latter value is significantly smaller than the damping ratio $k_1(\pi/4) = 233.9\text{m}^{-1}$. The dependences $F_1(r)$ in figure 5a, b almost coincide with each other,

whereas the dependences $F_{\lambda}(r)$ in these figures are different. The damping ratio near the inner sphere in Figure 5a depends on the meridional angle and it is close to zero in the middle radial part of the layer. Thus, at the considered two-frequency oscillations of the inner sphere, not only the low-frequency mode is enhanced but also its radial propagation direction from the inner sphere to the outer

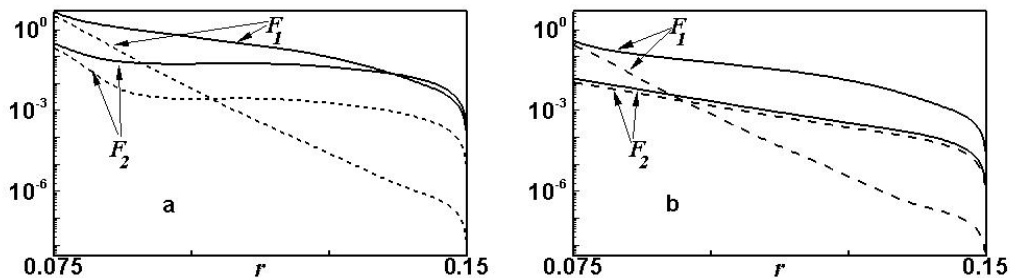


Figure 5. Radius dependence of the amplitudes at $\theta=\pi/2$ solid lines and at $\theta=\pi/4$ dashed lines.

(a) - two-frequency oscillations: $f_1 = 0.5\text{s}^{-1}$, $A_1 = 5\text{s}^{-1}$ and $f_2 = 0.07\text{s}^{-1}$, $A_2 = 0.2\text{s}^{-1}$; (b) - independent harmonic oscillations with the parameters of the high- and low-frequency modes.

one changes to the meridional propagation direction from the equator to a pole along the outer sphere. The modes are again spatially separated: the low- and high-frequency waves propagate in the regions adjacent to the outer and inner spheres, respectively.

4. Discussion of the results

The enhancement of the low-frequency mode in the flow at an increase in the amplitude of the high-frequency mode in the rotational velocity signal can be considered as manifestation of energy transfer from smaller scales to larger scales in the process of nonlinear interaction between the modes. Energy transfer from smaller scales to larger scales is similar to processes in quasi-two-dimensional turbulence. An inverse energy transfer cascade characteristic of quasi-two-dimensional turbulence was previously observed in a spherical layer at the periodic modulation of the rotation velocity of the inner sphere [9] in the frequency range limited from below by the modulation frequency and from above by the sphere rotation frequency. A significant difference of the flow formed at two-frequency oscillations of the inner boundary with respect to the rest state from the flow considered in [9] is the absence of the mean flow in the azimuthal direction and any instabilities. A common property of these flows is the presence of averaged large-scale meridional circulations. In our case, it is single-vortex circulation directed from the poles to the equator of the inner sphere.

The intensity of meridional circulation at small-amplitude oscillations is low. The behavior of both modes is similar to that at the corresponding harmonic oscillations (see figure 2d); i.e., the interaction between modes is absent. Because of the difference between the damping ratios, the high-frequency mode prevails near the inner sphere as a source of oscillations, whereas the low-frequency mode prevails far from the source of oscillations near the outer sphere; the interface between these two regions coincides with the contours of equal amplitudes of the modes (figure 2b). When the amplitude of the high-frequency mode in the signal of sphere velocity increases, the intensity of circulation increases by an order of magnitude, the radial velocity near the equator increases by two orders of magnitude, and the equatorial jet turns near the equator of the outer sphere, as is indicated by wave surfaces, e.g., in figure 1b and figure 4a. Such an intense flow in the meridional plane significantly changes the damping ratios of the azimuthal component of the velocity. The damping ratios near the equatorial plane decrease significantly (see figure 5a) because fluid acquiring a high kinetic energy near the inner sphere is rapidly transferred to the region adjacent to the outer sphere. However, the low-frequency mode prevails near the outer sphere and this mode is enhanced.

Thus, circulation in the meridional plane plays a decisive role in energy transfer from smaller scales to larger scales. In particular, the enhancement of the low-frequency mode is due to intense meridional circulation, which is in turn enhanced at an increase in the amplitude of any mode in the

rotation signal. A feature of the meridional circulation is its presence in any flow limited by rotating spherical boundaries: in wide and very thin layers, at the rotation of only the inner boundary, and at the unidirectional rotation of both spherical boundaries. Large-scale meridional circulation exists in the Earth's atmosphere [12]. Since the enhancement of the low-frequency mode is, as mentioned above, due to intense circulation, this is the reason to expect that the enhancement of the low-frequency mode considered in this work can be manifested in large-scale geo flows.

5. Conclusions

The results of the numerical studies have shown that a flow in a spherical layer at two-frequency rotational oscillations of the inner sphere with respect to the rest state is separated into two regions. The high- and low-frequency modes dominate near the inner and outer spheres, respectively. The position of the boundary between the regions is independent of time and coincides with amplitude contours of oscillations at each of the modes. The waves with small amplitudes are spherical as in the case of periodic oscillations with wave surfaces perpendicular to the radius. With an increase in the amplitude of the high-frequency mode in the signal of the velocity of the sphere, the division of the flow into two regions holds, but the wave structure of the flow, as well as the ratio of the amplitudes of the low- and high-frequency modes, changes. The direction of propagation of the wave in the region adjacent to the outer sphere changes from radial to meridional and the low-to-high-frequency mode amplitude ratio increases. The considered phenomenon is the energy transfer from high-frequency velocity oscillations with the larger amplitude to the low-frequency mode with the smaller amplitude. The energy transfer between the modes involves a meridional circulation and the unsteady flow remains stable in this case. The excess of the amplitude of the low-frequency mode over the amplitude of the high-frequency mode increases with a decrease in the low frequency and depends significantly on the meridional angle: it increases by two orders of magnitude from the equator to the pole.

Acknowledgments

This work was supported by the Russian Foundation for Basic Research project no. 160500004. MG acknowledges support from the ERC Advanced Grant No. 320773, and the Russian Foundation for Basic Research, project no. 16-07-01072. Research at the Ural Federal University is supported by the Act 211 of the Government of the Russian Federation, agreement No 02.A03.21.0006.

References

- [1] Noir J, Hemmerlin E, Wicht J, Baca S M, and Aurnou J M 2009 *Phys. Earth Planet Inter.* **173** 141
- Sturrock P A, Buncher J B, Fischbach E, Gruenwald J T, Javorsek D, Jenkins J H, Lee R H, Mattes J J, and Newport J R 2010 *Solar Phys.* **267** 251
- [2] Bryan G 1889 *Phil. Trans. London* **180** 187
- Staquet C and Sommeria 2002 *J. Ann. Rev. Fluid Mech.* **34** 559
- [3] Zhilenko D Yu and Krivososova O E 2015 *Dokl. Phys.* **60**
- [4] Sidorenkov N S 2004 *Herald Russ. Acad. Sci.* **74** 402
- [5] Phillips O M 1981 *J. Fluid Mech.* **106** 215
- Zakharov V E and Shamin R V 2010 *JETP Lett.* **91** 62
- Talipova T G, Pelinovsky E N and Kharif K 2011 *JETP Lett.* **94** 182
- [6] Nikitin N 2006 *J. Comp. Phys.* **217** 759
- [7] Zhilenko D Yu and Krivososova O E 2015 *Tech. Phys. Lett.* **41**, 5
- [8] Zhilenko D Yu and Krivososova O E and Nikitin N V 2007 *Fluid Dyn.* **42**, 886
- [9] Zhilenko D Yu and Krivososova O E 2015 *JETP Lett.* **101**, 527
- [10] Zinov'ev A L and Filippov L I 1975 *Introduction to the Theory of Signals and Circuits* (Moscow: Vyssh. Shkola) p 319
- [11] Landau L D and Lifshitz E M 1986 *Fluid Mechanics* (Moscow: Nauka) p 534
- [12] Gill A E 1982 *Atmosphere-Ocean Dynamics* (Cambridge: Academic) p 208